

UNCLASSIFIED

CENTRAL RESEARCH LIBRARY
DOCUMENT COLLECTION

MARTIN MARIETTA ENERGY SYSTEMS LIBRARIES



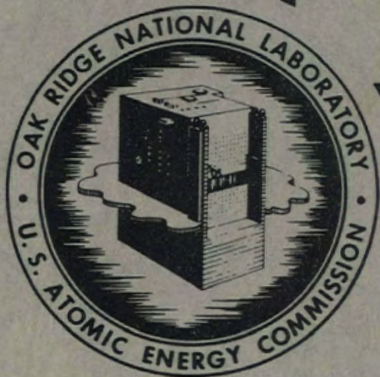
3 4456 0350305 5

ORNL-2164
Physics *cy. 97*

A FLUX DEPRESSION EXPERIMENT

IN THE MTR

J. B. Trice



CENTRAL RESEARCH LIBRARY
DOCUMENT COLLECTION

LIBRARY LOAN COPY

DO NOT TRANSFER TO ANOTHER PERSON

If you wish someone else to see this document,
send in name with document and the library will
arrange a loan.

OAK RIDGE NATIONAL LABORATORY

OPERATED BY

UNION CARBIDE NUCLEAR COMPANY

A Division of Union Carbide and Carbon Corporation



POST OFFICE BOX P • OAK RIDGE, TENNESSEE

UNCLASSIFIED

Printed in USA. Price 30 cents. Available from the

Office of Technical Services
U. S. Department of Commerce
Washington 25, D. C.

LEGAL NOTICE

This report was prepared as an account of Government sponsored work. Neither the United States, nor the Commission, nor any person acting on behalf of the Commission:

- A. Makes any warranty or representation, express or implied, with respect to the accuracy, completeness, or usefulness of the information contained in this report, or that the use of any information, apparatus, method, or process disclosed in this report may not infringe privately owned rights; or
- B. Assumes any liabilities with respect to the use of, or for damages resulting from the use of any information, apparatus, method, or process disclosed in this report.

As used in the above, "person acting on behalf of the Commission" includes any employee or contractor of the Commission to the extent that such employee or contractor prepares, handles or distributes, or provides access to, any information pursuant to his employment or contract with the Commission.

UNCLASSIFIED

ORNL-2164

Contract No. W-7405-eng-26

SOLID STATE DIVISION

A FLUX DEPRESSION EXPERIMENT IN THE MTR

J. B. Trice

DATE ISSUED

OCT 9 1956

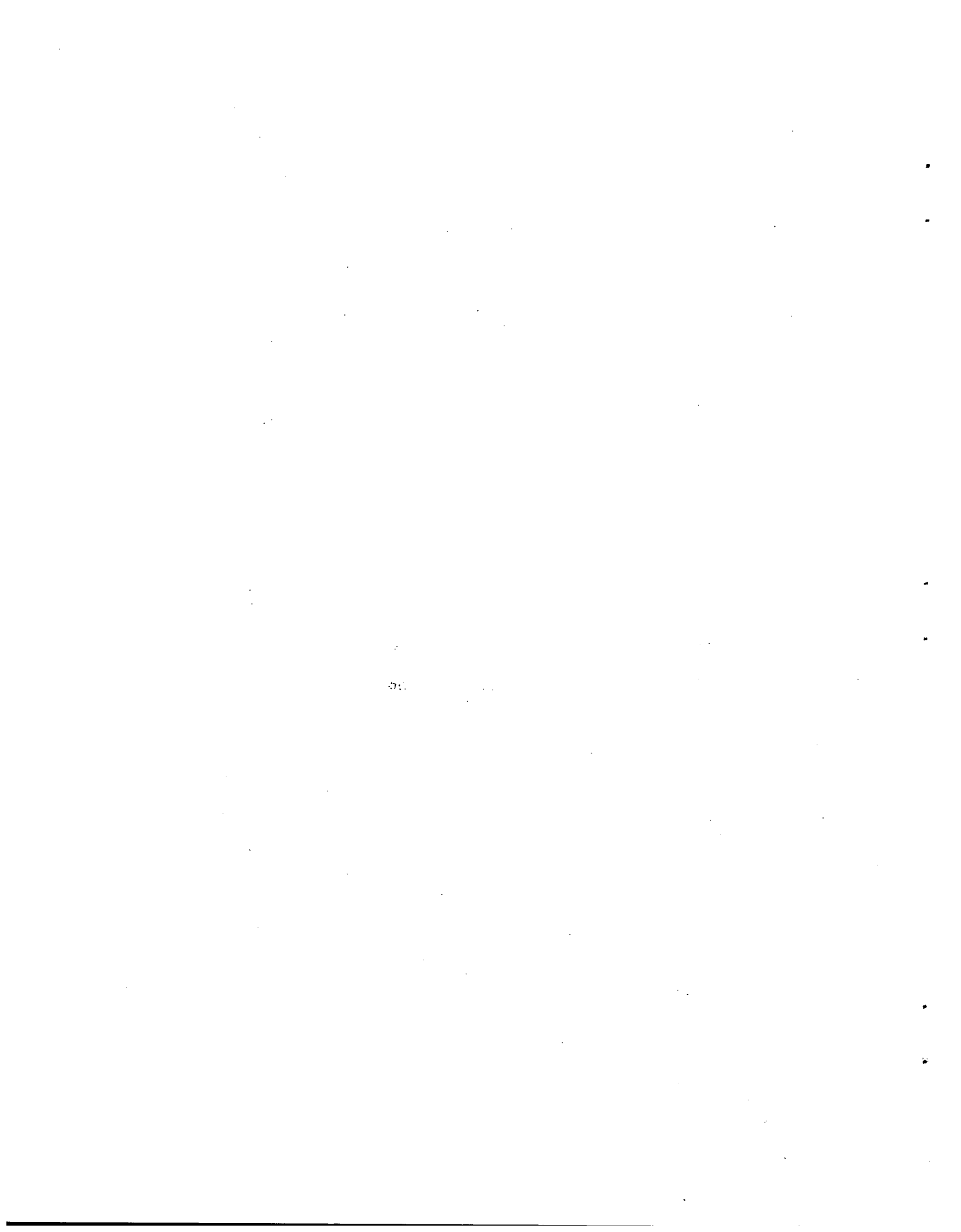
OAK RIDGE NATIONAL LABORATORY
Operated by
UNION CARBIDE NUCLEAR COMPANY
A Division of Union Carbide and Carbon Corporation
Post Office Box P
Oak Ridge, Tennessee

MARTIN MARIETTA ENERGY SYSTEMS LIBRARIES



3 4456 0350305 5

UNCLASSIFIED



INTERNAL DISTRIBUTION

1. C. D. Baumann
2. R. G. Berggren
3. J. O. Betterton, Jr.
4. D. S. Billington
5. D. Binder
6. T. H. Blewitt
7. E. P. Blizard
8. A. L. Boch
9. C. D. Bopp
10. B. S. Borie
11. G. E. Boyd
12. H. Brooks (consultant)
13. W. E. Browning
14. W. E. Brundage
15. A. D. Callihan
16. D. W. Cardwell
17. R. M. Carroll
18. C. E. Center (K-25)
19. R. A. Charpie
20. J. W. Cleland
21. C. E. Clifford
22. A. F. Cohen
23. D. D. Cowen
24. J. H. Crawford, Jr.
25. S. J. Cromer
26. F. L. Culler
27. J. E. Cunningham
28. R. R. Dickison
29. S. E. Dismuke
30. L. B. Emler (K-25)
31. W. K. Ergen
32. J. H. Frye, Jr.
33. J. L. Gabbard
34. R. J. Gray
35. W. O. Harms (consultant)
36. C. S. Harrill
37. L. B. Holland
38. A. Hollaender
39. D. K. Holmes
40. A. S. Householder
41. J. T. Howe
42. L. K. Jetter
43. R. J. Jones
44. W. H. Jordan
45. G. W. Keilholtz
46. C. P. Keim
47. R. B. Lindauer
48. P. M. Reyling
49. M. T. Kelley
50. F. L. Keller
51. R. H. Kernohan
52. E. M. King
53. T. A. Lincoln
54. S. C. Lind
55. R. S. Livingston
56. W. D. Manly
57. F. C. Maienschein
58. C. J. McHargue
59. A. J. Miller
60. E. C. Miller
61. J. G. Morgan
62. K. Z. Morgan
63. J. P. Murray (Y-12)
64. M. L. Nelson
65. R. B. Oliver
66. W. W. Parkinson
67. R. W. Peelle
68. A. M. Perry
69. M. T. Robinson
70. E. S. Schwartz
71. H. C. Schweinler
72. E. D. Shipley
73. O. Sisman
74. M. J. Skinner
75. G. P. Smith
76. A. H. Snell
77. R. L. Sproull (consultant)
78. E. E. Stansbury
79. D. K. Stevens
80. C. D. Susano
81. J. A. Swartout
82. E. H. Taylor
83. D. B. Trauger
84. J. M. Warde
85. C. C. Webster
86. M. S. Wechsler
87. R. A. Weeks
88. W. R. Willis (consultant)
89. A. M. Weinberg
90. E. P. Wigner (consultant)
91. G. C. Williams
92. J. C. Wilson
93. C. E. Winters
94. M. C. Wittels
95. Biology Library
96. Health Physics Library

- 97-98. Central Research Library
99-118. Laboratory Records Department
119. Laboratory Records, ORNL R.C.
120. Reactor Experimental
Engineering Library
121. ORNL - Y-12 Technical Library,
Document Reference Section

EXTERNAL DISTRIBUTION

122. R. F. Bacher, California Institute of Technology
123. Division of Research and Development, AEC, ORO
124. W. H. Shaver, Corning Glass Works, Corning, New York
125. S. H. Liebson, Naval Research Laboratory, Washington, D.C.
126. W. C. Sears, University of Georgia
127. R. L. Doan, Phillips Petroleum Company
128. H. V. Klaus, Phillips Petroleum Company
129. M. Fox, Brookhaven National Laboratory
130. J. R. Johnson, Minnesota Mining and Manufacturing Co., St. Paul
131. J. B. Trice, Operations Analysis, Headquarters, SAC, Offutt Air Force
Base, Nebraska
132. R. N. Little, ANP Project Office, Fort Worth
133. G. L. Stiehl, Convair Division of General Dynamics Corp., San Diego
134-730. Given distribution as shown in TID-4500 under Physics category

DISTRIBUTION PAGE TO BE REMOVED IF REPORT IS GIVEN PUBLIC DISTRIBUTION

List of Figures

- Fig. 1 Lattice Loading of MTR During Period of Flux-Depression Study
- Fig. 2 Alloy Rods and Holder Assemblies for Measuring Flux Depression
- Fig. 3 Effective Values of Perturbed Flux vs Amount of Cadmium in Absorber Rod
- Fig. 4 Thermal-Flux Depression vs Amount of Cadmium in Core
- Fig. 5 Thermal-Neutron Flux vs Reactor Power
- Fig. 6 Average Shim-Rod Position for MTR in March 1955
- Fig. 7 Thermal-Neutron Flux in Core vs Wall Thickness of Holder
- Fig. 8 An Effective Thermal-Flux Axial Traverse Along HB-3
- Fig. 9 Thermal-Flux Traverse Through "Light Grey" Absorber in HB-3 High-Flux Zone
- Fig. 10 Perturbed and Unperturbed Flux Traverses from Inside to "Walled Holder" by Using Three Different Neutron Absorbers in High-Flux Zone
- Fig. 11 Perturbed and Unperturbed Flux Traverses Inside 1/16-in.-Wall Holder by Using Two Different Neutron Absorbers in Low-Flux Zone
- Fig. 12 Flux-Depression Curve for a 1/8-in.-Wall Holder
- Fig. 13 Perturbed and Unperturbed Flux Traverses Inside a 3/16-in.-Wall Holder
- Fig. 14 Perturbed and Unperturbed Flux Traverses Inside a 1/4-in.-Wall Holder
- Fig. 15 Unperturbed Thermal-Flux Traverse for HB-3
- Fig. 16 Thermal Flux Measured with Co^{60} Along the HB-3 Axis with R-11 Position Partially Shadow Shielded
- Fig. 17 Diagram Showing Sectioning of Alloy Rod for Chemical Analysis
- Fig. 18 External Part of ORNL Pneumatic Facility at MTR
- Fig. 19 Shuttle-Train Assembly for ORNL Pneumatic Facility at MTR

List of Tables

- Table 1 Calibration Data to Relate Thermal-Neutron Flux to Reactor Power
- Table 2 Flux-Depression Data for 10-Min Irradiation at Position Beginning 13.1 In. from End of Pneumatic Tube and with Reactor at 30 Mw.
- Table 3 Flux-Depression Data for Irradiations at High-Flux End of Pneumatic Tube
- Table 4 Flux-Depression Data for Eight Different Alloys with Varying Weight Percentages of Cadmium and with Reactor at 5 Mw
- Table 5 Chemical Analyses of Samples Listed in Tables 2, 3, and 4
- Table 6 Flux-Depression Data for Eight Different Compositions of Cd-Mg Rods
- Table 7 Chemical Analyses of Samples from Section No. 1 and Listed in Table 6
- Table 8 Chemical Analyses of Samples from Section No. 5 and Listed in Table 6
- Table 9 Chemical Analyses of Samples from Sections No. 2 or No. 4 and Listed in Table 6
- Table 10 Chemical Analyses of Samples from Section No. 3 and Listed in Table 6

Summary

Thermal-neutron flux intensities were measured in the interior of several solid, cylindrical rods inserted into an MTR beam hole. Variables that were studied included both the functional dependence of cross section on neutron energy and the extent of absorption -- "greyness" of neutron absorber. It was found that the first variable has only a small effect on flux depression in the rod. The second variable, "greyness," has a large effect, and for this reason, a graphical relation between absorber "greyness" and thermal-flux reduction was established.

A FLUX DEPRESSION EXPERIMENT IN THE MTR

Introduction

Many of the experiments in the MTR require some estimate of the effective thermal-neutron flux in or near the experimental assemblies. In one of the MTR beam holes, currently assigned to ORNL for fast-neutron spectral studies, an opportunity arose whereby the effectiveness of neutron absorbers in reducing thermal flux could be determined. Since simple theoretical estimates of the quantity which involves flux depression and self absorption are impractical to make, especially when complicated geometries are involved, experimental data of the type to be described is of considerable importance to anyone who must either design in-pile experiments or interpret results from such experiments.

The setting for the group of measurements to be described is illustrated in Fig. 1, which shows a schematic picture of the HB-3 hole and its physical location with respect to the MTR lattice. The axis of the beam hole lies in approximately the horizontal-lattice mid-plane.

Results

The thermal-neutron flux was measured through the interior of a cylindrical assembly containing the neutron absorber and consisting of two major pieces. The outer piece was an Inconel cylinder 7 in. in length and was hollow so that a solid rod of the neutron absorber could be inserted. The solid absorber consisted of two halves of a cylinder which had been sliced along its axis and was slotted at intervals in such a way as to allow cobalt foils to be located along the axis in intimate contact with the absorber material (See Fig. 2). The variables studied were the effects on flux diminution caused by variations in the inner cylinder composition (macroscopic cross section), the container wall thickness, and the position along axis of HB-3.

To exhibit the relationship between strength of neutron absorber and the effective neutron flux within the absorber, Figures 3 and 4 present data which encompass an interval from almost complete white (no absorption) to almost complete black (complete absorption). The data were obtained by using eight different compositions of cadmium-magnesium alloy. In Fig. 3, the effective flux values are normalized to the unperturbed value for the flux; that is, the measurement was obtained with no mockup inside of the pneumatic tube. Figure 4 shows a curve which is based on the same data except that the per cent depression is normalized to the flux in an essentially empty Inconel tube.

The relationship of reactor power to thermal flux is shown in Fig. 5. A nonlinear relationship between reactor power and thermal flux is indicated above 20 Mw. Other work⁽¹⁾ also corroborates these data. Control-rod position seems to have only a small effect, if any, on the thermal-flux level in HB-3, and therefore the nonlinear relationship is thought to be due to factors other than this. Figure 6 shows average control-rod position for the most important period during which the experimental work was carried out. The relation between power and flux was obtained because many of the irradiations were made with the reactor operating at five Mw in order to limit the intensity of gamma heat. At 30 Mw the core materials would have melted for many of the irradiations -- an unacceptable situation.

The effect of wall thickness on the flux in the absorber core is shown in Fig. 7. The abscissa is $R_2^2 - R_1^2$ where $R_2 - R_1$ (the top abscissa) is the wall thickness. Wall thicknesses range from 1/16 in. to 1/4 in., and core absorbers include alloys containing both cadmium and boron.

(1) Pratt and Whitney Aircraft Corp., private communication with G. U. Parks, April 27, 1955.

Figure 8 represents a composite picture of the effective flux as measured with three different core compositions and identical Inconel tube containers with 1/16-in. walls. Both the perturbed and unperturbed flux measurements extend about 20 in. along the axis of HB-3. Although there appear to be no discernable differences in depression among the three cores represented, calculations,⁽²⁾ based on a thermal-neutron absorption cross section of 3500 barns for cadmium, show that the effective flux in the core is not a sensitive function of core composition but, rather, is governed strongly by the average absorption cross section of the entire assembly.

Figure 9 shows flux measurements at the high-intensity location that were taken through the absorber core for a weakly absorbing alloy containing 0.574 wt % cadmium ($0.187 \text{ cm}^2/\text{cc}$).⁽²⁾ The absorber was contained in a standard-type Inconel cylinder with 1/16-in.-thick wall.

Figure 10 shows similar traverses for a cadmium-bearing material, a boron-bearing material, and a lithium-bearing material with macroscopic absorption cross sections at 0.025 ev. of $2.1 \text{ cm}^2/\text{cc}$, $2.7 \text{ cm}^2/\text{cc}$ and $1.5 \text{ cm}^2/\text{cc}$, respectively. As in Fig. 9, these traverses represent the high-flux intensity region and were run in Inconel tubes with a 0.269-in. ID, a 1/16-in.-wall thickness and which were closed at both ends.

Figures 11 through 14 show measurements taken with cadmium- and boron-containing materials over a lower-intensity neutron-flux region than the previous figures. Also, the relationship between depression and wall thickness is obtained from this series of measurements. The walls of the Inconel tube range from 1/16 in. to 1/4 in.; and as in all of the measurements for this experiment, the inside diameter of the Inconel cylinders is 0.269 in.

Figure 15 shows a traverse of unperturbed thermal-neutron flux obtained with cobalt samples placed in a light magnesium four-train shuttle in the HB-3 hole,

(2) K. Way et al., Nuclear Data, NBS-499 (Sept. 1, 1950)

and Fig. 16 shows another traverse that is identical except that the first point was partially shadow-shielded by an Inconel cup which contained the cobalt for the first position. A comparison of these two curves indicates that the shadowing effect was small.

Tables

Most of the tables contain all of the data necessary to convert the radio-activity readings of the cobalt to thermal-flux values.

In Table 1, under the column entitled Sample, 2.5 R11 means that the reactor instruments read 2.5 Mw and that the measurement was carried out in position R11. Sample 220 R11 means the second measurement at 20 Mw in position R11. When the shuttle train is fully inserted, position R11 is 2.6-in. from the external end of the beam-hole; and subsequent positions, such as R12, R13, etc., are spaced at two-in. intervals. The remainder of Table 1 is obvious.

In Table 2, a code was used to designate the sample; thus for sample LH2A0 the significance of each numerical and alphabetical symbol is given in its proper sequence.

Absorber --- 1 refers to the first absorber; 2 refers to the first preparation of cadmium; 3 refers to the second group of cadmium cores.

Inconel Wall Thickness --- H is 1/16 in.; G is 1/8 in.; F is 3/16 in.; E is 1/4 in.

Tube Number --- 2 refers to the second Inconel tube in the H series.

Position of cobalt foil --- A designates the first position for the cobalt foil; B is the second position; etc. (See Fig. 2).

Location of cobalt foil with respect to Inconel tube --- O means that the foil is on the outside surface of the Inconel tube; N means it is inside; X means it is between the cap and the core.

The reading in volts is a direct reading from the 4π γ -ray ionization chamber at the MTR. The reading corrected to the 10^{10} scale of the instrument is shown, and this number can be converted into dis/sec of Co^{60} by multiplying the volts obtained on the 10^{10} scale by 0.76×10^6 , which is the calibration factor for the instrument. Near the end of Table 2 are a group of data designated as MH2A0, etc.; M simply refers to the fact that the Inconel tube was empty.

In Table 3, MH in the code identifies an empty tube with an H-size wall thickness. In the group 6G2A0, etc., 6 designates a particular cadmium-containing alloy. Below this group, the data are given for samples which were irradiated in a solid-beryllium parallelepiped about 7-in. long. The beryllium was used in an attempt to increase the effective thermal flux by moderating the fast neutrons in the hole. (3) Although no increase in flux was observed, it is thought that in some cases moderation by beryllium may be used to help offset effects of flux depression. The group of runs beginning CD5HA0, etc. were additional measurements with cadmium cores; but for this group, the end of the Inconel tube which pointed away from the reactor core was sawed off. The next group is a set of data for boron cores, and the group following it is a series of measurements in which empty magnesium shuttles were used and in which position R11 was partially shadowed. Here the cobalt in R11 was contained in a "cup" made from the end of the Inconel tube that was sawed off for the CD5H group. The final two measurements in Table 3 are for the lithium-base core. They were made in an H-size tube.

Table 4 is a compilation of data obtained with an H-size tube which contained a core with varying amounts of cadmium and which was in the high-intensity zone. Note that the ratio of fluxes at 30 Mw and at 5 Mw for this run is 6.68 and is not the smaller number (< 5) measured previously. (4)

(3) Recent unpublished measurements in HB-3 indicate that the fast-neutron intensity is too low to contribute significantly to the thermal-neutron flux by means of moderation in beryllium.

(4) See Fig. 5.

Table 5 shows a tabulation of important quantities for calculating points in the curves given in Figs. 3 and 4.

Table 6 contains in summary form the data for the alloys of varying composition. The positions A, B, C, and D refer to the locations shown in Fig. 9 for the sequence of points from left to right. (See explanation of codes used.) This table is better analyzed by reference to Figs. 3 and 4, which show the most important results graphically.

Chemical analyses of alloy rods are shown in Table 7 through 10. Several sections for analysis were taken on both sides of the piece of stock that was used for the actual sample fabrication. A diagram of a typical alloy rod is shown in Fig. 17 and the sections sampled are indicated.

Apparatus

The equipment for inserting the samples into the HB-3 beam hole is shown in Figs. 18 and 19. Figure 18 shows the external part of the ORNL pneumatic facility which is a device for the semiautomatic irradiation and unloading of threshold detectors used in the measurement of fast neutron fluxes -- operations which at times require counting within a minute or so after irradiation. For the present experiment however, the facility was manually operated since the shape of the Inconel tubes was not adaptable to the automatic features of the facility. In order to load an Inconel tube, the cups were removed from the "hot" end of the shuttle train shown in Fig. 19. Then the tube fitted easily into the shuttle car and was loaded into the runway. A stiff aluminum wire attached to the outer end of the shuttle train was used to insert and remove the sample assembly. After each 10-min irradiation at 5 Mw, the train was withdrawn from the flux zone into the reactor shield at a point where it could be "sensed" by a "cutie pie" next to the reactor shield. Here it was allowed to "cool" for about an hour before it was removed into a nearby lead shield on the floor. During the removal of the tube to the shield the radiation level at

about 18 in. (length of the tongs used) was approximately 10 to 50 roentgens per hour. However, this phase was performed swiftly in order to minimize the total biological dose. Readings from finger rings and film badges later showed that personnel had stayed within prescribed tolerance limits. Since the half life of Co^{60} is 5.1 years, there was no urgent need to remove the samples from the Inconel tubes, and thus several days were allowed for a "cooling-off" period. By this time, the radiation level near the tubes was only a few milliroentgens per hour, and it was possible to proceed with the final disassembly, removal, weighing, and counting of the samples.

Errors

In the calculations, no attempt was made to correct for the fact that the effective temperature of the neutrons was perhaps 100°C higher than room temperature (0.025 ev) nor was a correction made to take into account the Maxwellian neutron-distribution effect, which would lower the effective cross section of the thermal neutrons to about 89% of its listed value. These corrections can be made if desired. Internal errors occurred in connection with weighing, counting, and positioning the samples during irradiation. It is thought that the total of all these errors is less than 10%. Also, associated with the measurement of absolute fluxes were some constant errors; namely, errors associated with the cross section and the half life of Co^{60} , and with the calibration of the 4π gamma-ionization chamber. These add another 10% to single measurements of absolute flux, but it must be emphasized that all of the flux depression results were based on relative measurements, whereas the actual flux measurements were absolute.

Acknowledgments

Thanks are due J. A. Milko, J. H. Coobs and J. H. Erwin of the ORNL Metallurgy Division for the fabrication and extrusion of the experimental alloys used in the tests.

D. R. Cuneo and W. R. Grimes of the ORNL Analytical Chemistry Division synthesized the lithium-containing materials.

F. Gourley, P. Monson and A. Vander Does weighed and counted the samples.

APPENDIX*

Absorption coefficient, μ_a^{**} (cm²/cc)

Inconel -----	0.37
Cadmium A and B -----	2.1
Boron Material -----	2.7
Lithium Material -----	1.5
Cadmium, Light Grey --	0.19

Density, ρ (g/cc)

Inconel -----	8.43
Cadmium A and B -----	1.72
Boron Material -----	2.7
Cadmium Light Grey ---	1.74

Cross Section, σ_a (barns)

Cadmium -----	3500
Boron -----	718
Lithium -----	67

* These data were useful throughout the report.

**
$$\mu \text{ Average} = \frac{\mu_a(\text{core})(r_2^2 - r_1^2) + \mu_a(\text{tube})(r_3^2 - r_2^2)}{r_3^2}$$

TABLE 1

CALIBRATION DATA TO RELATE THERMAL-NEUTRON FLUX TO REACTOR POWER

Sample	Thermal Flux ($\text{nv} \times 10^{-13}$)	Reactor Power (Mw)	Date	Time
2.5 R11	2.96	2.5	3-11-55	0935
2.5 R14	0.89	2.5	3-11-55	0935
3 R11	3.00	2.6	3-11-55	0950
3 R14	0.80	2.6	3-11-55	0950
5 R11	5.15	5.0	3-11-55	1015
15 R14	1.62	1.50	3-11-55	1015
15 R11	15.0	15.0	3-11-55	1327
15 R14	4.97	15.0	3-11-55	1327
20 R14	16.49	20.0	3-11-55	1400
220 R11	21.5	20.0	3-11-55	1515
220 R14	7.05	20.0	3-11-55	1515
30 R11	24.9	30.0	3-12-55	1100
30 R14	6.82	30.0	3-12-55	1100

Sample	Thermal Flux ($\text{nv} \times 10^{-14}$)	Reactor Power (Mw)	Control Rods, average for four rods (inches withdrawn)
230 R11	1.63	30	
230 R14	0.45	30	
330 R11	2.26	30	
330 R14	0.97	30	
430 R11	2.09	30	23.880
430 R14	0.64	30	23.880
530 R11	2.24	30	26.120
530 R14	0.69	30	26.120
730 R11	2.37	30	27.125
730 R14	0.72	30	27.125

Table 1 (Continued)

Sample	Thermal Flux ($\text{nv} \times 10^{13}$)	Reactor Power (Mw)
35 R11	29.6	35
35 R14	9.5	35
40 R11	33.6	40
40 R14	10.3	40

TABLE 2

DATA FOR 10-MINUTE IRRADIATIONS AT POSITION BEGINNING 13.1 IN. FROM END OF PNEUMATIC TUBE AND WITH REACTOR AT 30 Mw

Sample	Core	Weight (mg)	Activity (v)	Ionization Chamber Scale	Activity (v), Corrected to 10 ¹⁰ Scale	Thermal Flux (nv x 10 ⁻¹²)	Date
1H2A0	Boron	20.6	0.102	10 ¹⁰	7.75 x 10 ⁴	4.36	2-25-55
1H2AN	Boron	20.7	0.102	10 ¹⁰	7.75 x 10 ⁴	4.33	2-25-55
1H2BN	Boron	18.5	0.702	10 ¹¹	5.56 x 10 ⁴	3.48	2-25-55
1H2CN	Boron	15.4	0.499	10 ¹¹	3.92 x 10 ⁴	2.94	2-25-55
1H2DN	Boron	16.9	0.473	10 ¹¹	3.71 x 10 ⁴	2.55	2-25-55
2H2A0	Cd-A	20.8	0.160	10 ¹⁰	1.22 x 10 ⁵	6.81	2-24-55
2H2B0	Cd-A	19.1	0.115	10 ¹⁰	8.74 x 10 ⁴	5.30	2-24-55
2H2C0	Cd-A	11.6	0.790	10 ¹¹	6.27 x 10 ⁴	6.28	2-24-55
2H2AN	Cd-A	8.1	0.434	10 ¹¹	3.40 x 10 ⁴	2.87	2-24-55
2H2BN	Cd-A	9.4	0.384	10 ¹¹	3.0 x 10 ⁴	3.70	2-24-55
2H2CN	Cd-A	9.0	0.302	10 ¹¹	2.3 x 10 ⁴	3.00	2-24-55
2H2DN	Cd-A	11.3	0.356	10 ¹¹	2.77 x 10 ⁴	2.84	2-24-55
3H3A0	Cd-B	47.2	0.354	10 ¹⁰	2.69 x 10 ⁵	6.61	2-25-55
3H3B0	Cd-B	30.4	0.160	10 ¹⁰	1.21 x 10 ⁵	4.62	2-25-55
3H3C0	Cd-B	66.4	0.384	10 ¹⁰	2.92 x 10 ⁵	5.10	2-25-55
3H3AN	Cd-B	11.4	0.702	10 ¹¹	5.565 x 10 ⁴	5.66	2-25-55
3H3BN	Cd-B	24.7	0.101	10 ¹¹	7.676 x 10 ⁴	3.60	2-25-55
3H3CN	Cd-B	11.0	0.380	10 ¹¹	2.957 x 10 ⁴	3.12	2-25-55
3H3DN	Cd-B	23.1	0.654	10 ¹¹	5.176 x 10 ⁴	2.60	2-25-55
2G2A0	Cd-A	37.1	0.268	10 ¹⁰	2.04 x 10 ⁵	6.37	2-25-55
2G2B0	Cd-A	11.0	0.529	10 ¹¹	4.16 x 10 ⁴	4.38	2-25-55

TABLE 2 (CONTINUED)

Sample	Core	Weight (mg)	Activity (v)	Ionization Chamber Scale	Activity (v), Corrected to 10^{10} Scale	Thermal Flux ($\text{nv} \times 10^{-12}$)	Date
2G2CO	Cd-A	34.0	0.197	10^{10}	1.50×10^5	5.12	2-24-55
2G2AN	Cd-A	6.4	0.298	10^{11}	2.3×10^4	4.16	2-24-55
2G2BN	Cd-A	12.8	0.425	10^{11}	3.33×10^4	3.02	2-24-55
2G2CN	Cd-A	7.5	0.211	10^{11}	1.60×10^4	2.47	2-24-55
2G2DN	Cd-A	7.7	0.198	10^{11}	1.49×10^4	2.25	2-24-55
2F2AO	Cd-A	22.0	0.156	10^{10}	1.18×10^5	6.22	2-24-55
2F2BO	Cd-A	12.8	0.700	10^{11}	5.55×10^4	5.03	2-25-55
2F2CO	Cd-A	29.2	0.865	10^{11}	6.89×10^4	2.74	2-25-55
2F2AN	Cd-A	14.3	0.540	10^{11}	4.25×10^4	3.45	2-25-55
2F2BN	Cd-A	10.2	0.286	10^{11}	2.2×10^4	2.51	2-24-55
2F2CN	Cd-A	11.3	0.273	10^{11}	2.09×10^4	2.13	2-25-55
2F2DN	Cd-A	10.8	0.228	10^{11}	1.73×10^4	1.85	2-24-55
3F3AO	Cd-B	29.1	0.190	10^{10}	1.44×10^5	5.74	2-25-55
3F3BO	Cd-B	23.6	0.122	10^{10}	9.27×10^4	4.55	2-25-55
3F3CO	Cd-B	27.1	0.114	10^{10}	8.66×10^4	2.71	2-25-55
3F3AN	Cd-B	23.3	0.872	10^{11}	6.94×10^4	3.46	2-25-55
3F3BN	Cd-B	7.0	0.206	10^{11}	1.55×10^4	2.56	2-25-55
3F3CN	Cd-B	33.2	0.712	10^{11}	5.65×10^4	1.97	2-25-55
3F3DN	Cd-B	32.4	0.628	10^{11}	4.96×10^4	1.77	2-25-55
2E2AO	Cd-A	54.3	0.307	10^{10}	2.33×10^5	4.98	2-25-55
2E2BO	Cd-A	44.0	0.192	10^{10}	1.46×10^5	3.85	2-25-55
2E2CO	Cd-A	29.2	0.115	10^{10}	8.74×10^4	3.47	2-25-55

TABLE 2 (CONTINUED)

Sample	Core	Weight (mg)	Activity (v)	Ionization Chamber Scale	Activity (v), Corrected to 10^{10} Scale	Thermal Flux ($nv \times 10^{-12}$)	Date
2E2AN	Cd-A	18.1	0.544	10^{11}	4.28×10^4	2.74	2-25-55
2E2BN	Cd-A	9.6	0.216	10^{11}	1.63×10^4	1.97	2-25-55
2E2CN	Cd-A	7.6	0.147	10^{11}	1.07×10^4	1.64	2-25-55
2E2DN	Cd-A	7.8	0.137	10^{11}	0.99×10^4	1.47	2-25-55
3E3AO	Cd-B	44.3	0.255	10^{10}	1.94×10^5	5.07	2-25-55
3E3BO	Cd-B	17.1	0.750	10^{11}	5.95×10^4	4.04	2-25-55
3E3CO	Cd-B	53.0	0.190	10^{10}	1.44×10^5	3.16	2-24-55
3E3AN	Cd-B	21.9	0.693	10^{11}	5.50×10^4	0.201	2-24-55
3E3BN	Cd-B	31.1	0.564	10^{11}	4.45×10^4	0.165	2-25-55
3E3CN	Cd-B	30.3	0.659	10^{11}	5.22×10^4	0.200	2-25-55
3E3DN	Cd-B	24.6	0.387	10^{11}	3.02×10^4	0.143	2-24-55
MH2AO	None	20.4	0.180	10^{10}	1.37×10^5	0.780	2-28-55
MH2BO	None	14.7	0.858	10^{11}	6.87×10^4	0.540	2-28-55
MH2AN	None	15.5	0.154	10^{10}	1.17×10^5	0.880	2-28-55
MH2BN	None	17.0	0.868	10^{11}	6.95×10^4	0.47	2-28-55
MG2AO	None	18.8	0.938	10^{11}	7.52×10^4	0.46	2-28-55
MG2BO	None	12.3	0.938	10^{11}	7.44×10^4	0.70	2-28-55
MG2AN	None	25.5	0.109	10^{10}	8.28×10^4	0.38	2-28-55
MG2BN	None	25.7	0.199	10^{10}	1.51×10^5	0.68	2-28-55
MF2AO	None	23.4	0.160	10^{11}	1.22×10^5	0.60	2-28-55
MF2BO	None	24.5	0.112	10^{10}	8.51×10^4	0.40	2-28-55
MF2AN	None	11.3	0.762	10^{11}	6.09×10^4	0.63	2-28-55

TABLE 2 (CONTINUED)

Sample	Core	Weight (mg)	Activity (v)	Ionization Chamber Scale	Activity (v), Corrected to 10 ¹⁰ Scale	Thermal Flux (nv x 10 ⁻¹²)	Date
MF2BN	None	32.3	0.115	10 ¹⁰	8.74 x 10 ⁴	0.31	2-28-55
ME2AO	None	18.7	0.111	10 ¹⁰	8.44 x 10 ⁴	0.523	2-28-55
ME2AN	None	34.2	0.166	10 ¹⁰	1.26 x 10 ⁵	0.427	2-28-55
ME2BN	None	23.5	0.661	10 ¹¹	5.27 x 10 ⁴	0.260	2-28-55
1E3AO	Boron	16.0	0.938	10 ¹¹	7.52 x 10 ⁴	0.55	2-28-55
1E3AX	Boron	26.1	0.283	10 ¹⁰	2.15 x 10 ⁵	0.96	2-28-55
1E3AN	Boron	16.8	0.525	10 ¹¹	4.17 x 10 ⁴	0.29	2-28-55
1E3BN	Boron	12.8	0.283	10 ¹¹	2.21 x 10 ⁴	0.20	2-28-55
1E3CN	Boron	12.1	0.231	10 ¹¹	1.79 x 10 ⁴	0.17	2-28-55
1E3DN	Boron	13.0	0.207	10 ¹¹	1.60 x 10 ⁴	0.14	2-28-55
1F1AO	Boron	14.9	0.906	10 ¹¹	7.26 x 10 ⁴	0.56	2-28-55
1F1AX	Boron	7.4	0.387	10 ¹¹	6.33 x 10 ⁴	0.99	2-28-55
1F1AN	Boron	10.4	0.387	10 ¹¹	3.05 x 10 ⁴	0.34	2-28-55
1F1BN	Boron	13.1	0.361	10 ¹¹	2.84 x 10 ⁴	0.25	2-27-55
1F1CN	Boron	12.5	0.272	10 ¹¹	2.12 x 10 ⁴	0.20	2-27-55
1F1DN	Boron	13.2	0.255	10 ¹¹	1.98 x 10 ⁴	0.17	2-28-55

TABLE 3

DATA FOR IRRADIATIONS AT HIGH-FLUX END OF PNEUMATIC TUBE

Sample	Core	Thermal Flux ($\text{nv} \times 10^{-14}$)	Reactor Power (Mw)
MH2A0	Empty	1.57	30
MH2B0	Empty	0.83	30
MH2AN	Empty	1.47	30
MH2BN	Empty	0.84	30
6G2A0	Cd-A	0.69	30
6G2AX*	Cd-A	1.81	30
6G2Nose	Cd-A	1.52	30
6H2A0	Cd-A	0.72	30
6H2AX	Cd-A	1.81	30

Sample	Weight (mg)	Exposure Time	Activity (v)	Ionization Chamber Scale	Activity (v), Corrected to 10^{10} Scale	Thermal Flux ($\text{nv} \times 10^{-14}$)	Date	Reactor Power (Mw)
Be-A	22.3	10 min	0.548	10^9	4.44×10^6	2.25	2/28/55	30
Be-B	12.8	10 min	0.100	10^9	7.54×10^5	0.70	2/28/55	30
Be-R21	11.2	10 min	0.583	10^{10}	4.44×10^5	0.47	2/28/55	30
Be-R23	13.6	10 min	0.26	10^{10}	1.98×10^5	0.17	2/28/55	30

Sample	Core	Weight (mg)	Exposure Time	Activity (v)	Ionization Chamber Scale	Activity (v), Corrected to 10^{10} Scale	Thermal Flux Normalized to 30 Mw ($\text{nv} \times 10^{-14}$)	Date	Reactor Power (Mw)
Cd5HA0	Cd-A	5.0	200 sec	0.945	10^{11}	7.53×10^4	2.33	3/12/55	5
Cd5HB0	Cd-A	9.3	200 sec	0.631	10^{11}	4.98×10^4	0.842	3/12/55	5

TABLE 3 (CONTINUED)

Sample	Core	Weight (mg)	Exposure Time	Activity (v)	Ionization Chamber Scale	Activity (v), Corrected to 10 ¹⁰ Scale	Thermal Flux Normalized to 30 Mw (nv x 10 ⁻¹⁴)	Date	Reactor Power (Mw)
Cd5HAN	Cd-A	5.8	200 sec	0.574	10 ¹¹	4.65 x 10 ⁴	1.21	3/12/55	5
Cd5HBN	Cd-A	6.3	200 sec	0.460	10 ¹¹	3.5 x 10 ⁴	0.882	3/12/55	5
Cd5HCN	Cd-A	7.6	200 sec	0.418	10 ¹¹	3.1 x 10 ⁴	0.680	3/12/55	5
Cd5HDN	Cd-A	11.6	200 sec	0.483	10 ¹¹	3.79 x 10 ⁴	0.522	3/12/55	5
B5H2AO	Boron	4.0	200 sec	0.772	10 ¹¹	6.13 x 10 ⁴	2.35	3/12/55	5
BH2BO	Boron	10.5	200 sec	0.756	10 ¹¹	6.87 x 10 ⁴	0.887	3/12/55	5
B5H2AN	Boron	9.5	200 sec	0.903	10 ¹¹	7.19 x 10 ⁴	1.37	3/12/55	5
B5H2BN	Boron	9.3	200 sec	0.673	10 ¹¹	5.33 x 10 ⁴	0.910	3/12/55	5
B5H2CN	Boron	8.7	200 sec	0.404	10 ¹¹	3.76 x 10 ³	0.589	3/12/55	5
B5H2DN	Boron	8.0	200 sec	0.414	10 ¹¹	3.23 x 10 ⁴	0.455	3/12/55	5
R11-H	-----	13.2	10 min	0.316	10 ⁹	2.69 x 10 ⁶	2.2	2/26/55	30
R12-H	-----	14.8	10 min	0.307	10 ⁹	2.47 x 10 ⁶	1.86	2/26/55	30
R14-H	-----	14.0	10 min	0.130	10 ⁹	9.42 x 10 ⁵	0.78	2/26/55	30
R21-H	-----	15.3	10 min	0.854	10 ¹⁰	4.31 x 10 ⁷	0.50	2/26/55	30
R22-H	-----	24.1	10 min	0.800	10 ¹⁰	6.18 x 10 ⁵	0.30	2/26/55	30

Sample	Core	Exposure Time	Position, distance from nose (in.)	Thermal Flux (nv x 10 ⁻¹³)	Date	Reactor Power (Mw)	Thermal Flux, (normalized to 30 Mw)(nv x 10 ⁻¹⁴)
D11	Lithium	200 sec	1.68	2.22	4/8/55	5.0	1.0
D12	Lithium	200 sec	3.09	1.40	4/8/55	5.0	0.63
D13	Lithium	200 sec	4.6	0.91	4/8/55	5.0	0.41
D14	Lithium	200 sec	5.4	0.76	4/8/55	5.0	0.34

* Core Melted

TABLE 4

Flux-Depression Data for Eight Alloys with Varying Weight Percentages of Cadmium and with Reactor at 5 Mw

Sample	Thermal Flux ($\text{nv} \times 10^{-13}$)	Date	Thermal Flux Normalized ^a to 30 Mw ($\text{nv} \times 10^{-14}$)	Power Factor ^b	Weight (mg)
A-H-A-N	2.60	6/20/55 ^c	1.74	6.68	28.0
A-H-B-N	1.98	6/20/55 ^c	1.32	6.68	40.1
A-H-C-N	1.51	6/20/55 ^c	1.01	6.68	27.7
A-H-D-N	1.14	6/20/55 ^c	0.75	6.68	8.8
A-H-R22	0.419	6/20/55 ^c	0.28	6.68	15.6
B-H-A-N	3.09	8/11/55	1.66	5.38	34.2
B-H-B-N	2.30	8/11/55	1.24	5.38	42.5
B-H-C-N	1.84	8/11/55	0.99	5.38	16.6
B-H-D-N	1.26	8/11/55	0.678	5.38	37.8
B-H-R22	0.521	8/11/55	0.28	5.38	25.6
C-H-A-N	2.59	8/11/55	1.48	5.73	57.9
C-H-B-N	2.04	8/11/55	1.17	5.73	36.4
C-H-C-N	1.57	8/11/55	0.9	5.73	22.1
C-H-D-N	1.13	8/11/55	0.494	5.73	29.5
C-H-R22	0.489	8/11/55	0.28	5.73	14.8
D-H-A	2.14	8/11/55	1.17	5.46	42.7
D-H-B	1.66	8/11/55	0.906	5.46	30.1
D-H-C	1.22	8/11/55	0.666	5.46	29.4
D-H-D	0.906	8/11/55	0.494	5.46	26.7
D-H-R22	0.513	8/11/55	0.28	5.46	20.0

TABLE 4 (CONTINUED)

Sample	Thermal Flux (nv x 10 ⁻¹³)	Date	Thermal Flux Normalized ^a to 30 Mw (nv x 10 ⁻¹⁴)	Power Factor ^b	Weight (mg)
E-H-A-N	1.61	8/11/55	8.92	5.54	29.3
E-H-B-N	1.14	8/11/55	0.632	5.54	36.5
E-H-C-N	0.854	8/11/55	0.474	5.54	26.7
E-H-D-N	0.634	8/11/55	0.352	5.54	23.8
E-H-R22	0.505	8/11/55	0.28	5.54	28.9
F-H-A-N	0.914	8/11/55	0.498	5.46	26.1
F-H-B-N	0.658	8/11/55	0.359	5.46	54.9
F-H-C-N	0.501	8/11/55	0.273	5.46	35.3
F-H-D-N	0.362	8/11/55	0.197	5.46	22.7
F-H-R22	0.513	8/11/55	0.28	5.46	26.8
G-H-A-N	0.417	8/11/55	0.231	5.54	23.8
G-H-B-N	0.288	8/11/55	0.16	5.54	39.9
G-H-C-N	0.185	8/11/55	0.103	5.54	26.9
G-H-D-N	0.139	8/11/55	0.0771	5.54	43.4
G-H-R22	0.505	8/11/55	0.28	5.54	53.5
H-H-A-N	0.355	8/11/55	0.194	5.46	32.5
H-H-B-N	0.243	8/11/55	0.0906	5.46	52.0
H-H-C-N	0.166	8/11/55	0.0775	5.46	23.5
H-H-R22	0.513	8/11/55	0.28	5.46	35.1

^a Position for normalization = R22

^b Power factor = $\frac{(\phi_{th})_{30 \text{ Mw}}}{(\phi_{th})_{5 \text{ Mw}}}$

^c Time removed - 0045 A.M.

TABLE 5

CHEMICAL ANALYSES⁵ OF A GROUP OF ABSORBER SAMPLES
 REPORTED IN TABLES 2, 3 AND 4

Sample	Method	Material Sought	Weight (%)
Boron-Containing	Gravimetric	Aluminum	93.37
			96.37
			96.96
			96.61
			96.52
	Potentiometric Titration	Boron	2.45
			2.51
			2.51
	Colorimetric	Iron	0.26
			0.28
Cadmium-Containing, A	Gravimetric	Magnesium	93.07
			93.39
			93.06
	Gravimetric	Cadmium	6.32
			6.43
			6.33
Cadmium-Containing, B	Gravimetric	Magnesium	93.51
			93.41
			93.55
		Cadmium	6.29
			6.29
			6.33

⁵ The analyses for cadmium and boron in their respective container materials were made under the supervision of J. Edgerton of the ORNL Analytical Chemistry Division.

TABLE 6

FLUX-DEPRESSION DATA FOR EIGHT DIFFERENT COMPOSITIONS OF Cd-Mg RODS

Position	Alloy							
	#1 (0.58 wt % Cd)	#2 (1.24 wt % Cd)	#3 (2.25 wt % Cd)	#4 (4.46 wt % Cd)	#5 (8.95 wt % Cd)	#6 (17.9 wt % Cd)	#7 (37.9 wt % Cd)	#8 (83.8 wt % Cd)
Monitor R22	2.8×10^{13}							
A	1.74×10^{14}	1.66×10^{14}	1.48×10^{14}	1.17×10^{14}	8.92×10^{13}	4.98×10^{13}	2.31×10^{13}	1.94×10^{13}
B	1.32×10^{14}	1.24×10^{13}	1.17×10^{14}	9.06×10^{13}	6.32×10^{13}	3.59×10^{13}	1.6×10^{13}	1.33×10^{13}
C	1.01×10^{14}	9.9×10^{13}	9.0×10^{13}	6.66×10^{13}	4.74×10^{13}	2.73×10^{13}	1.03×10^{13}	9.06×10^{13}
D	7.5×10^{13}	6.78×10^{13}	4.94×10^{13}	4.94×10^{13}	3.52×10^{13}	1.97×10^{13}	7.71×10^{12}	7.75×10^{12}

FLUX EXPRESSED AS PERCENT OF FLUX FOR ALLOY 1

A	100	95.4	85.0	67.2	51.2	28.6	13.3	11.2
B	100	94.0	88.5	68.6	47.9	27.4	12.1	10.2
C	100	98.0	89.1	65.9	46.9	27.0	10.2	8.97
D	100	90.5	86.4	65.9	47.0	26.3	10.3	10.3
		377.9	349.0	267.6	193.0	109.3	45.9	40.67
Average	100	100.0						
		94.5	87.3	66.9	48.3	27.6	11.5	10.2
Flux Depressed	0	5.5	12.7	33.1	51.7	72.4	88.5	89.8
				<u>PERCENT* OF UNPERTURBED FLUX</u>				
	79.0	74.8	69.0	52.9	38.2	21.8	9.1	8.06
Flux Depressed	21.0	25.2	31.0	47.1	61.8	78.2	90.9	91.94

* Average

TABLE 7
CHEMICAL ANALYSES OF SAMPLES FROM SECTION NO. 1

Alloy	Cadmium (Wt. %)	Magnesium (Wt. %)
1	0.88, 0.86, 0.87	99.87, 99.85, 99.80, 99.94
2	1.20, 1.24, 1.22	98.38, 99.09, 99.20, —
3	2.22, 2.21, 2.27	98.33, 98.26, 98.40 —
4	4.67, 4.61, 4.63	95.67, 95.92, 95.86 —
5	9.12, 9.09, 9.14	91.70, 91.70, 91.17 —
6	18.24, 18.15, 18.19	81.81, 81.85, 81.67 —
7	37.75, 38.91, 38.51	61.82, 61.79, 61.56 —
8	83.68, 83.87, 83.86	15.34, 15.47, 15.40, 15.25

TABLE 8
CHEMICAL ANALYSES OF SAMPLES FROM SECTION NO. 5

Alloy	Cadmium (Wt. %)	Magnesium (Wt. %)
1	0.78, 0.77, 0.77, ----	99.34, 99.96, 99.34
2	1.29, 1.33, 1.29, ----	99.47, 99.50, 99.56
3	2.36, 2.40, 2.42, 2.37	97.74, 97.74, 97.80
4	4.58, 4.58, 4.59, ----	96.65, 96.64, 96.56
5	9.24, 9.24, 9.24, ----	90.76, 90.82, 90.54
6	18.36, 18.42, 18.39, ----	81.61, 81.70, 81.58
7	38.16, 38.17, 38.32, 38.22	61.84, 61.56, 61.89
8	83.66, 83.94, 83.87, ----	15.25, 15.29, 15.22

TABLE 9
CHEMICAL ANALYSES OF SAMPLES FROM SECTION No. 2 OR NO. 4

Alloy	Cadmium (Wt. %)	Magnesium (Wt. %)
1	0.65, 0.66, 0.66, 0.65, 0.65	99.48, 99.66, 99.63, 99.89

TABLE 10
CHEMICAL ANALYSES OF SAMPLES FROM SECTION NO. 3

Alloy	Cadmium (Wt. %)	Magnesium (Wt. %)
1	.58, .58, .58 —	99.6, 100.0, — —
2	1.25, 1.23, 1.24 —	99.3, 98.6 — —
3	2.26, 2.25, — —	98.3, 98.2 — —
4	4.45, 4.48, 4.46 —	95.5, 96.2 — —
5	8.92, 8.97, 8.96 —	92.4, 92.8, 92.4 —
6	17.8, 18.0, 18.0, 17.8	82.5, 82.2, 82.2 —
7	37.8, 38.0, 38.1, 37.9	62.2, 62.1, 62.5, 62.2

UNCLASSIFIED
ORNL-LR-DWG 8636A

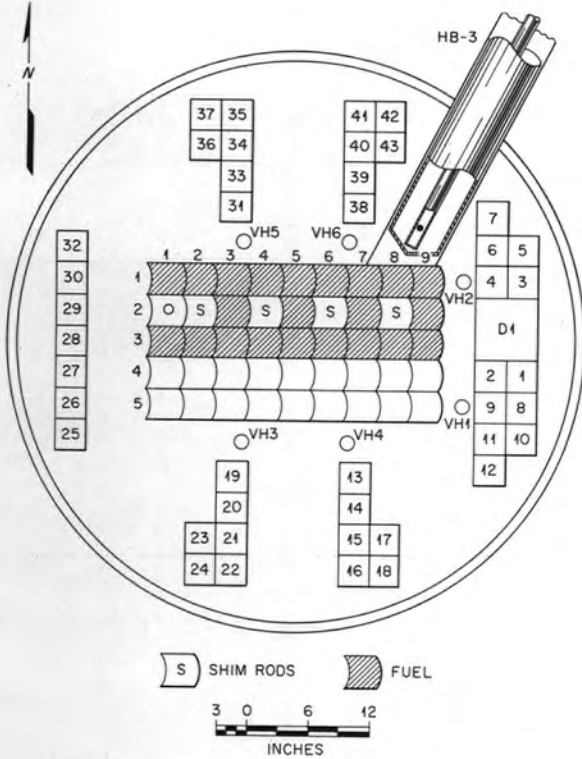


Fig. 1. Lattice Loading of MTR During Period of Flux-Depression Study.

UNCLASSIFIED
SSD-B-1294
ORNL-LR-DWG-9127

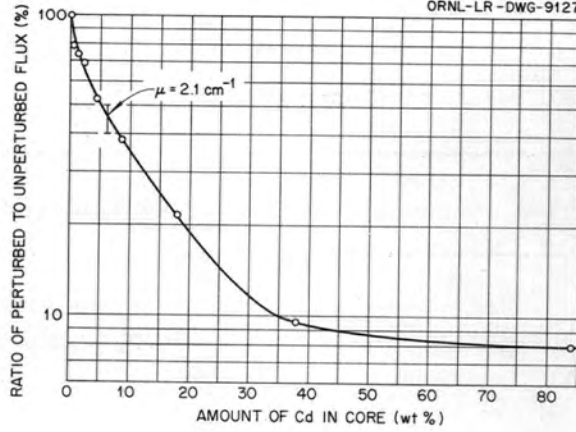


Fig. 3. Effective Values of Perturbed Flux vs Amount of Cadmium in Absorber Rod.

UNCLASSIFIED
PHOTO 15454

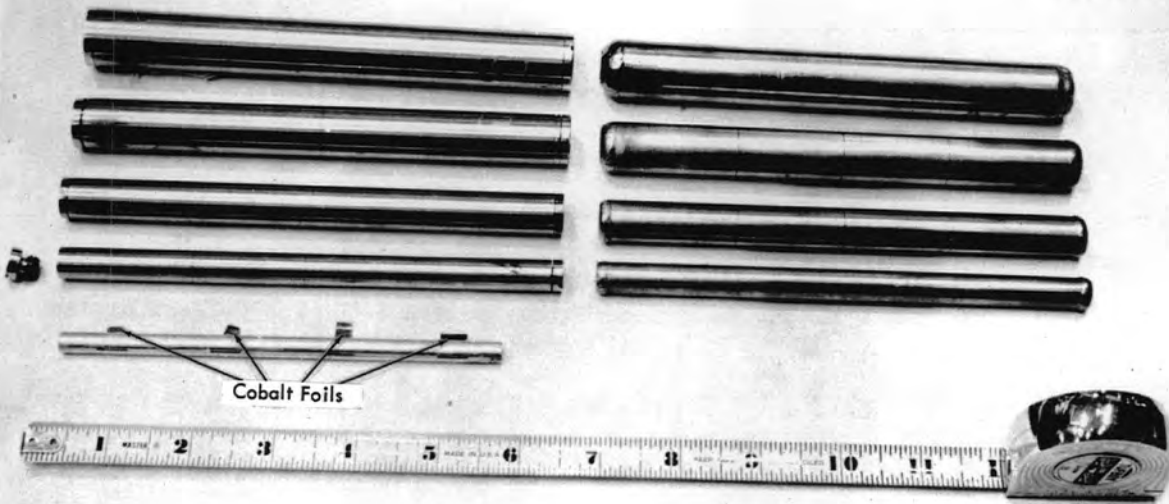


Fig. 2. Alloy Rods and Holder Assemblies for Measuring Flux Depression.

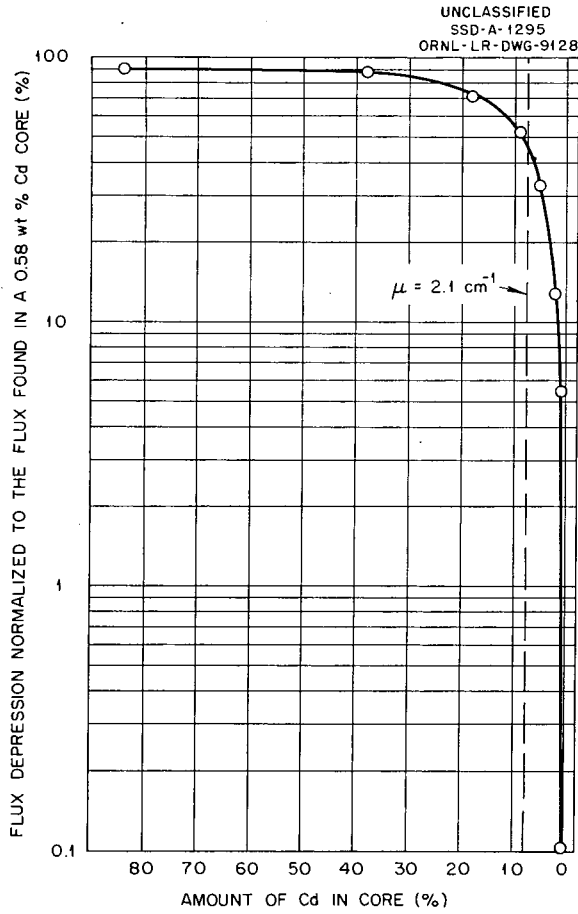


Fig. 4. Thermal-Flux Depression vs Amount of Cadmium in Core.

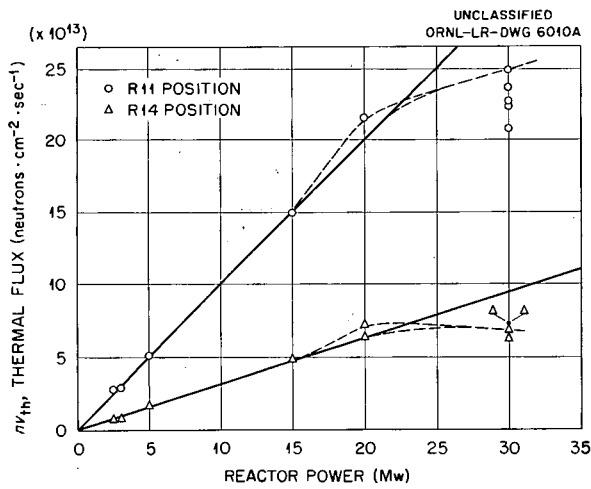


Fig. 5. Thermal-Neutron Flux vs Reactor Power.

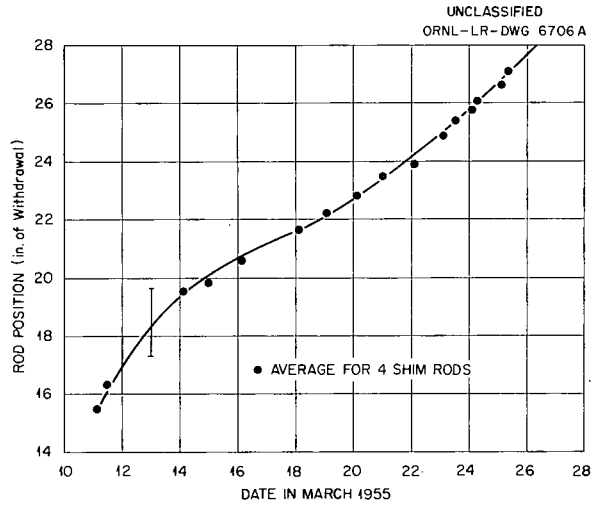


Fig. 6. Average Shim-Rod Position for MTR in March 1955.

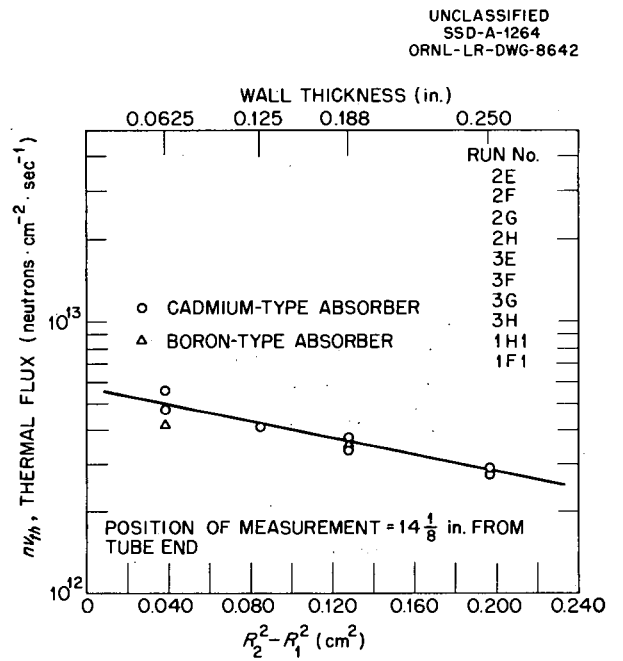


Fig. 7. Thermal-Neutron Flux in Core vs Wall Thickness of Holder.

UNCLASSIFIED
ORNL-LR-DWG 8832A

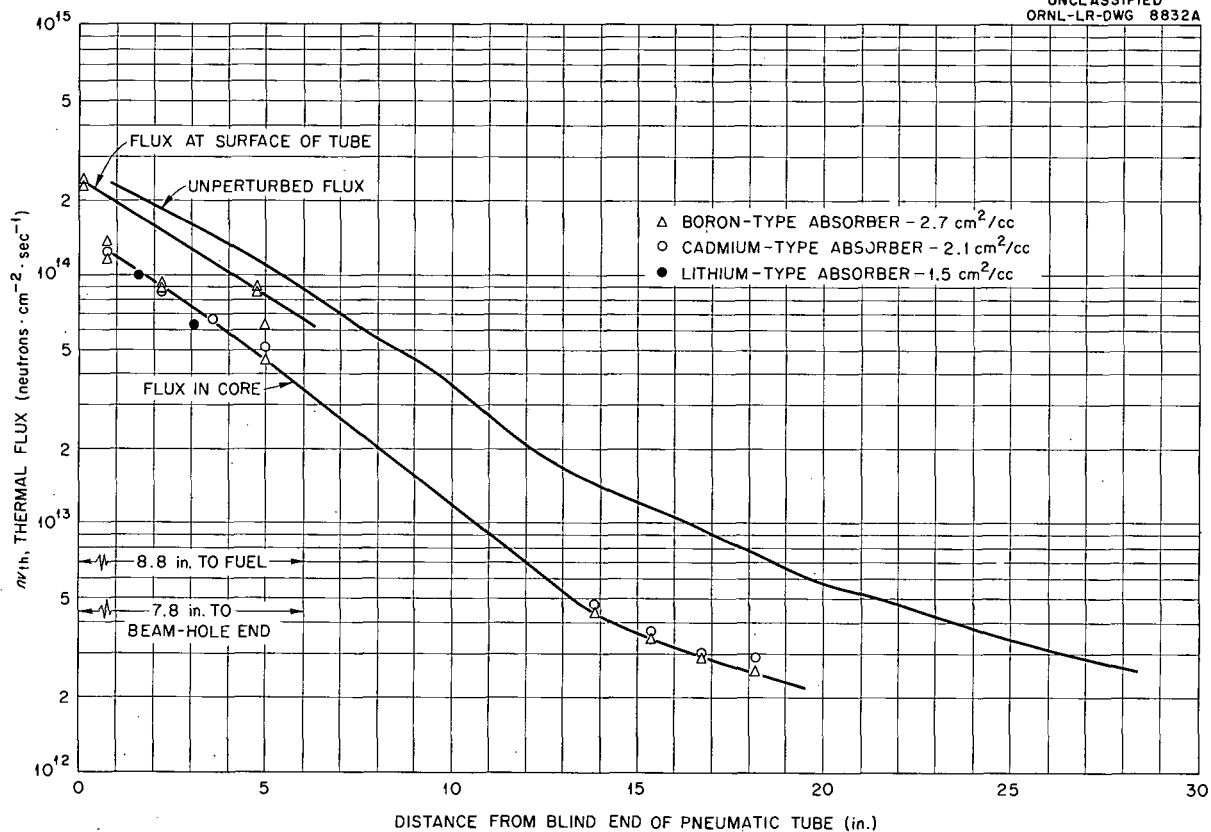


Fig. 8. An Effective Thermal-Flux Axial Traverse Along HB-3.

UNCLASSIFIED
SSD-A-1272
ORNL-LR-DWG-8829

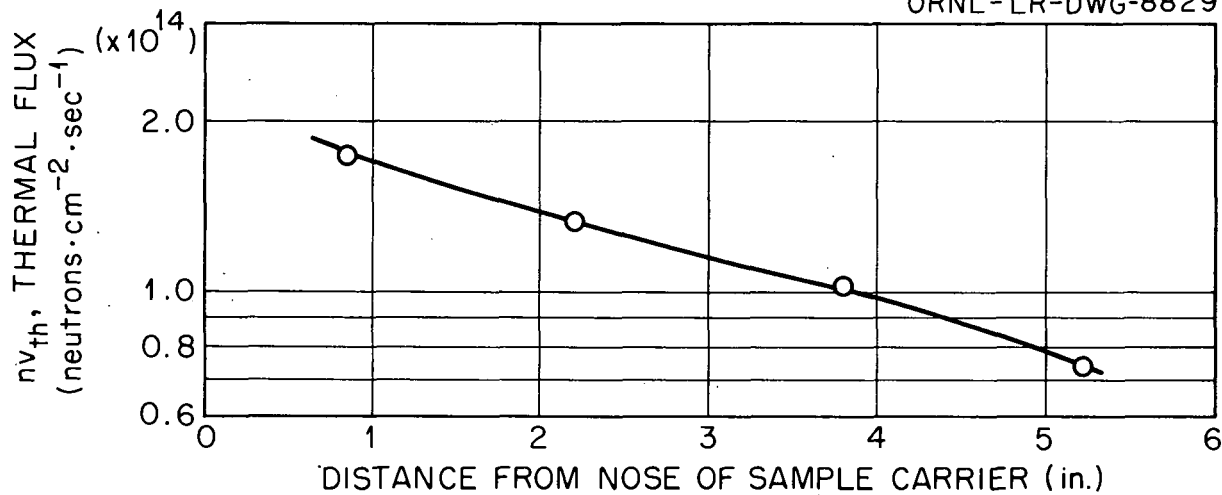


Fig. 9. Thermal-Flux Traverse Through "Light Grey" Absorber in HB-3 High-Flux Zone.

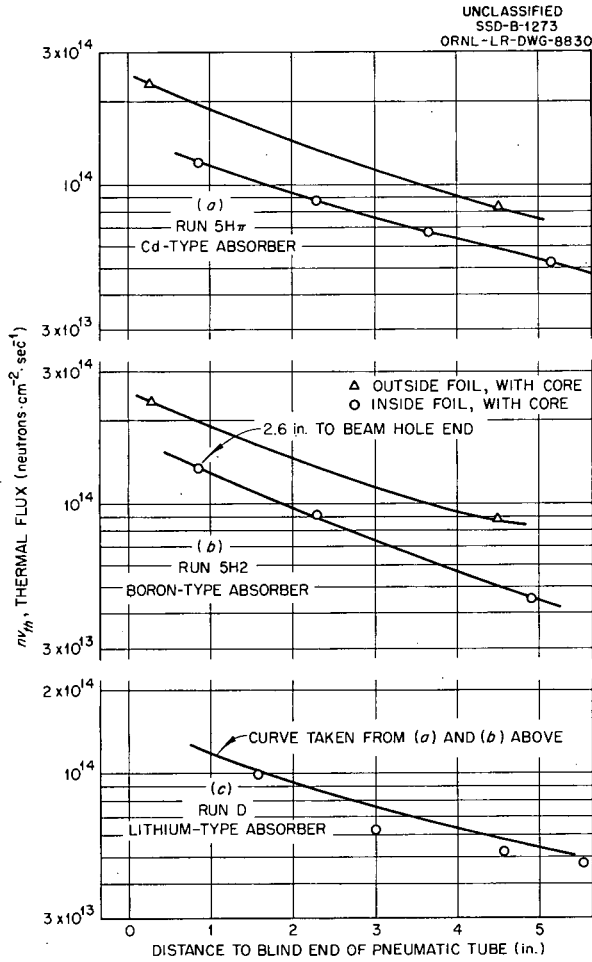


Fig. 10. Perturbed and Unperturbed Flux Traverses from Inside to "Walled Holder" by Using Three Different Neutron Absorbers in High-Flux Zone.

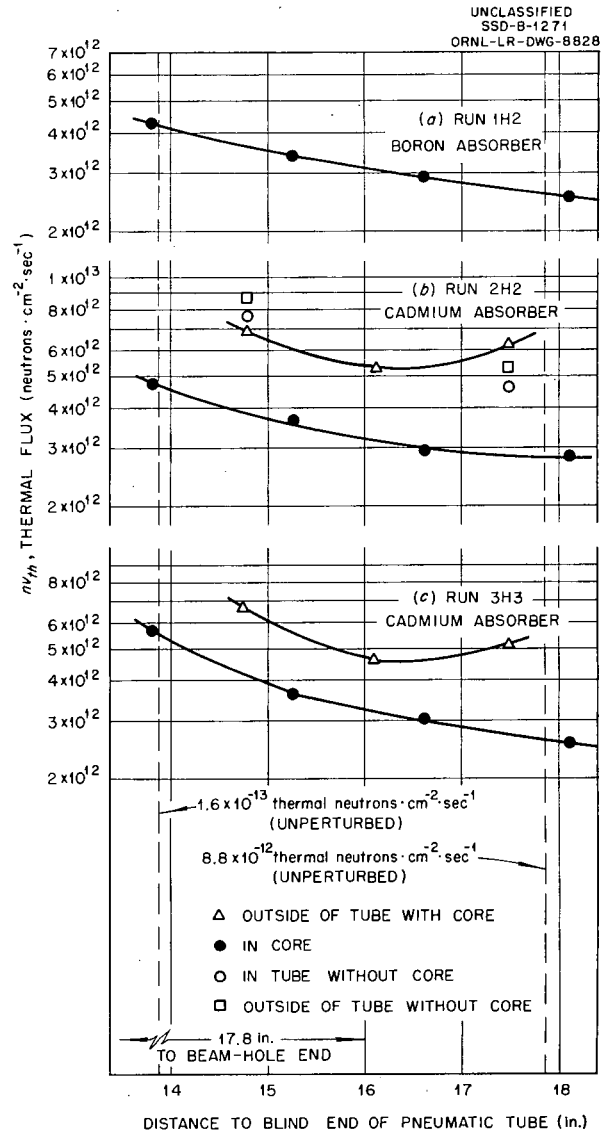


Fig. 11. Perturbed and Unperturbed Flux Traverses Inside 1/6-in.-Wall Holder by Using Two Different Neutron Absorbers in Low-Flux Zone.

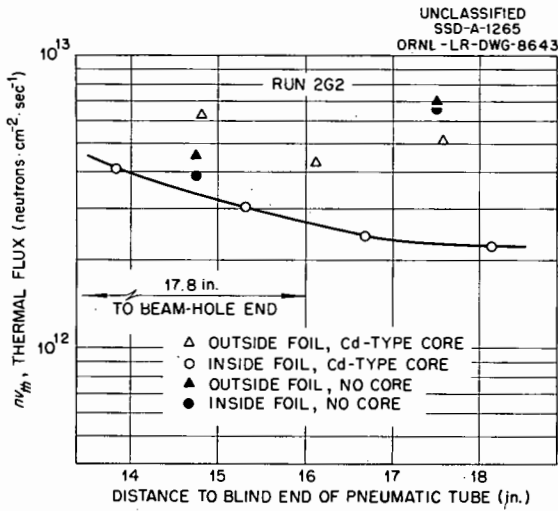


Fig. 12. Flux-Depression Curve for a $\frac{1}{8}$ -in.-Wall Holder.

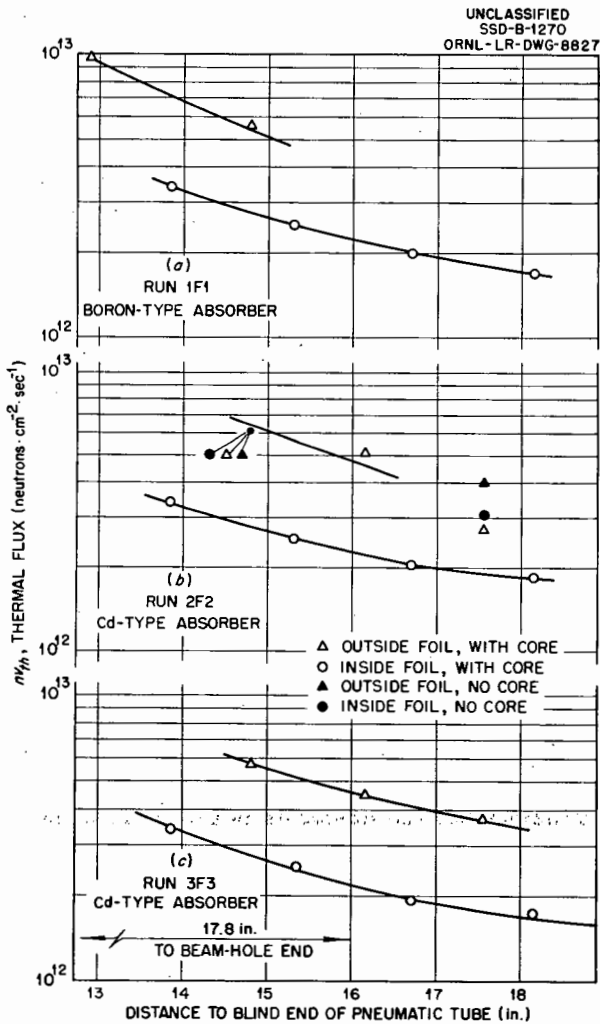


Fig. 13. Perturbed and Unperturbed Flux Trav-erses Inside a $\frac{3}{16}$ -in.-Wall Holder.

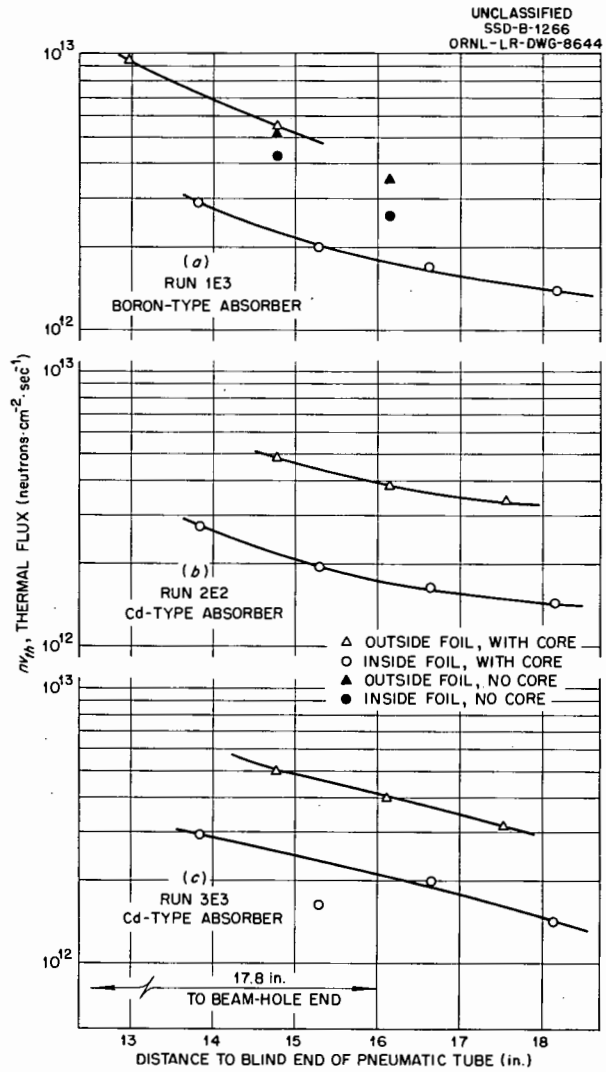


Fig. 14. Perturbed and Unperturbed Flux Trav-erses Inside a $\frac{1}{4}$ -in.-Wall Holder.

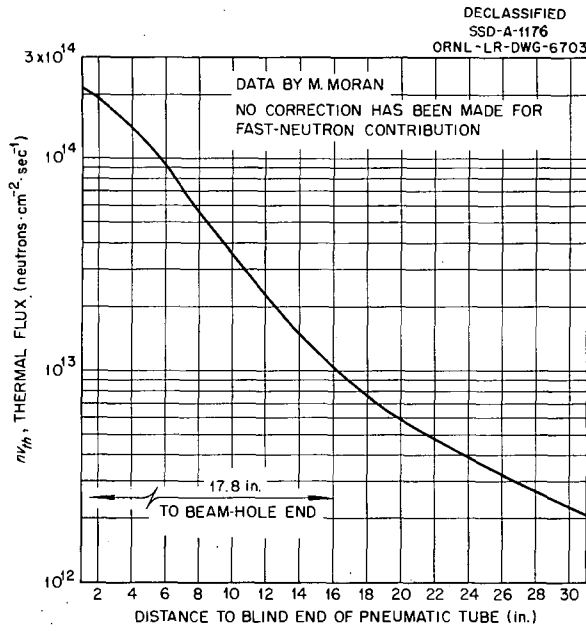


Fig. 15. Unperturbed Thermal-Flux Traverse for HB-3.

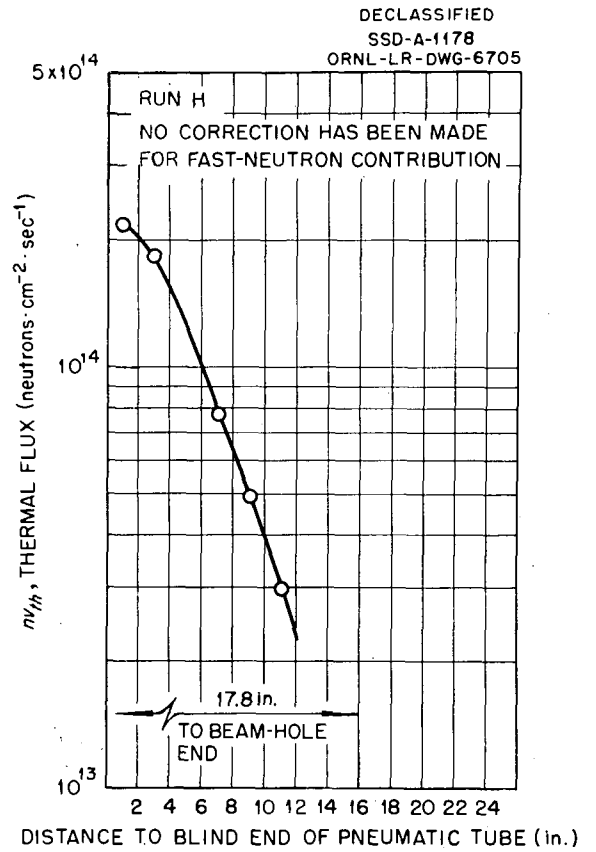


Fig. 16. Thermal Flux Measured with Co^{60} Along the HB-3 Axis with R-11 Position Partially Shadow Shielded.

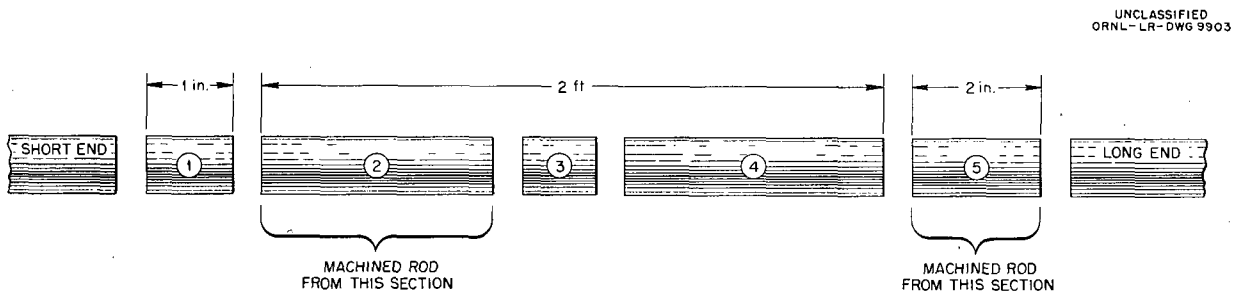


Fig. 17. Diagram Showing Sectioning of Alloy Rod for Chemical Analysis.

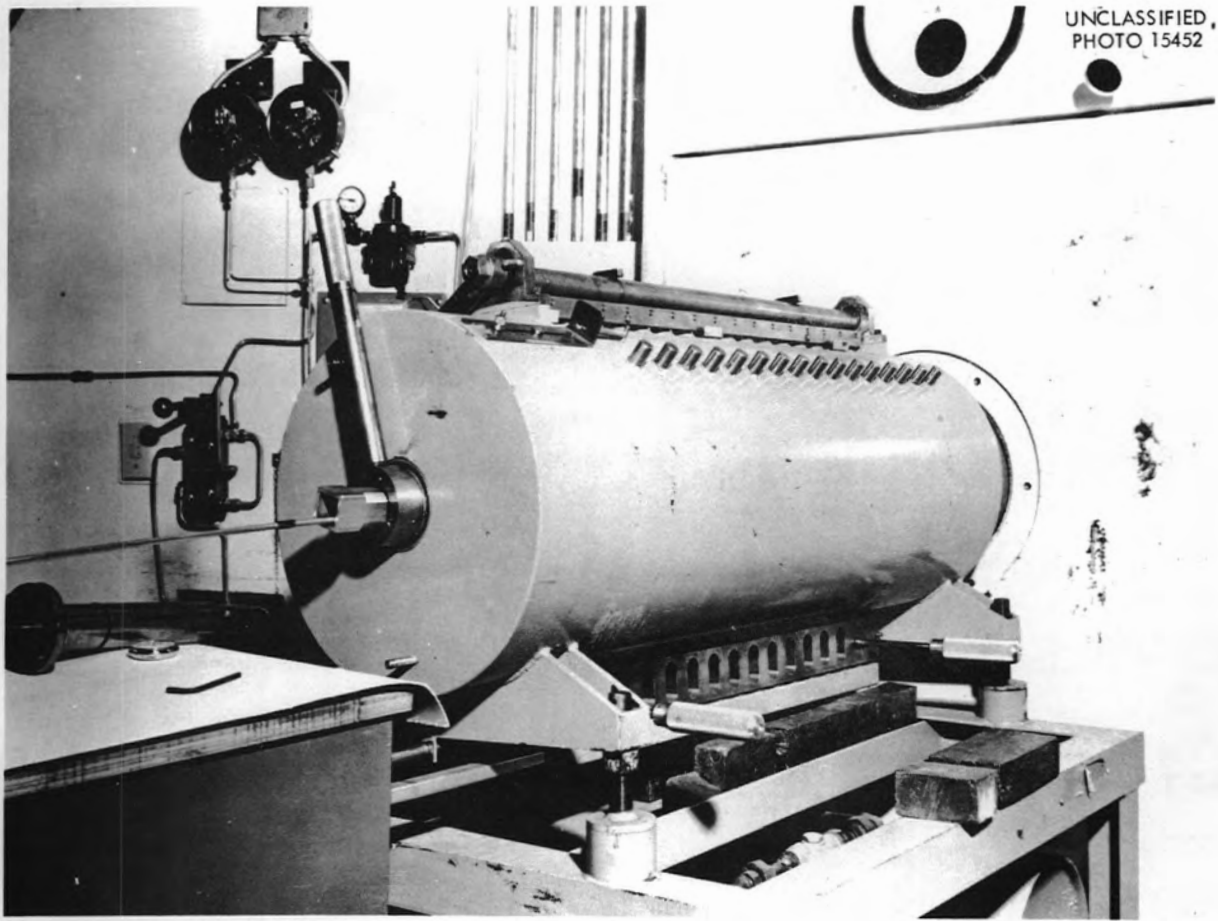


Fig. 18. External Part of ORNL Pneumatic Facility at MTR.

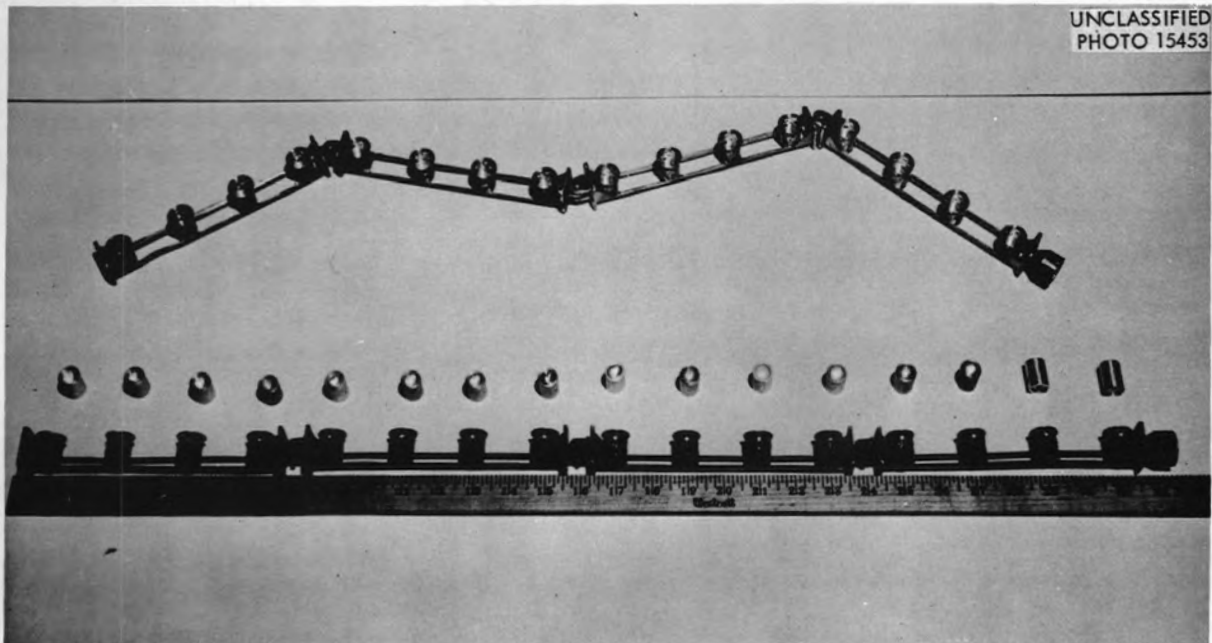


Fig. 19. Shuttle-Train Assembly for ORNL Pneumatic Facility at MTR.